

## Promoter Element Arising from the Fusion of Standard BioBrick Parts

Andrew I. Yao,<sup>†,‡,⊥</sup> Timothy A. Fenton,<sup>†,‡,⊥</sup> Keegan Owsley,<sup>†,‡,⊥</sup> Philip Seitzer,<sup>†,‡</sup> David J. Larsen,<sup>†,‡,||</sup> Holly Sit,<sup>‡</sup> Jennifer Lau,<sup>‡</sup> Arjun Nair,<sup>‡</sup> Justin Tantonloc,<sup>‡</sup> Ilias Tagkopoulos,<sup>‡,§</sup> and Marc T. Facciotti<sup>\*,†,‡</sup>

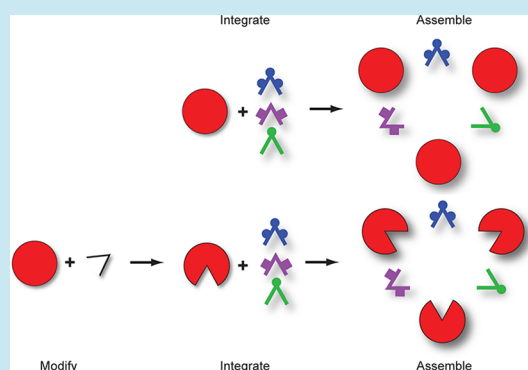
<sup>†</sup>Department of Biomedical Engineering, <sup>‡</sup>UC Davis Genome Center, and <sup>§</sup>Department of Computer Science, University of California Davis, One Shields Avenue, Davis, California 95616, United States

<sup>||</sup>Cellular and Molecular Biology Program, University of Michigan, 1011 North University Avenue, Ann Arbor, Michigan 48109, United States

### Supporting Information

**ABSTRACT:** We characterize the appearance of a constitutive promoter element in the commonly used *cI* repressor-encoding BioBrick BBa\_C0051. We have termed this promoter element pKAT. Full pKAT activity is created by the ordered assembly of sequences in BBa\_C0051 downstream of the *cI* gene encoding the 11 amino acid LVA proteolytic degradation tag, a BioBrick standard double-TAA stop codon, a genetic barcode, and part of the RFC10 SpeI-XbaI BioBrick scar. Placing BBa\_C0051 or other pKAT containing parts upstream of other functional RNA coding elements in a polycistronic context may therefore lead to the unintended transcription of the downstream elements. The frequent reuse of pKAT or pKAT-like containing basic parts in the Registry of Biological Parts has resulted in approximately 5% of registry parts encoding at least one instance of a predicted pKAT promoter located directly upstream of a ribosome binding site and ATG start codon. This example highlights that even seemingly simple modifications of a part's sequence (in this case addition of degradation tags and barcodes) may be sufficient to unexpectedly change the contextual behavior of a part and reaffirms the inherent challenge in carefully characterizing the behavior of standardized biological parts across a broad range of reasonable use scenarios.

**KEYWORDS:** synthetic biology, standard assembly, promoter, transcription, part characterization, iGEM, BioBrick



In the context of synthetic biology, a biological part can be defined as a bounded, functionally engineered, and contextually well-characterized element of DNA that abstracts sequence-level detail into a discrete qualitatively and quantitatively describable function.<sup>1</sup> An important corollary of part abstraction is the expectation that parts be functionally independent when they are used in specific operational and genetic contexts. Provided that contextual factors are accounted for, we assume that new functions should not arise unexpectedly from the element junctions between parts.

BioBrick and closely related parts definitions<sup>2,3</sup> have become a *de facto* standard in the field of synthetic biology. These standards have been popularized by the annual iGEM competition ([www.igem.org](http://www.igem.org))<sup>4</sup> but have also gained popularity outside of iGEM.<sup>5–10</sup> Most BioBrick parts are stored, validated, and distributed by the Registry of Standard Biological Parts ([www.partsregistry.org](http://www.partsregistry.org)),<sup>11</sup> which in addition to these roles serves to enforce part standardization. The ease of physical composability and accessibility of such parts has encouraged the reuse of standardized parts and part-based devices, in a variety of functional contexts.

Modifying parts, particularly protein-coding elements, through the addition of short 5' or 3' nucleotide extensions (typically encoding epitope tags, proteolytic degradation tags,

multiple stop codons, and barcodes) is a relatively common practice. These modifications add valuable functions to a part by simplifying a part's purification, enabling the *in vivo* or *in vitro* detection of an expressed protein product, changing a protein's degradation kinetics, or tracking the origin of a specific part. One could consider each of these modifying sequences as parts in their own right; each is an engineered DNA element that can, in the correct genetic context, add new desirable properties to other "part(s)" to which the tags are fused. However, since these tags are typically short, it is often easier to add the tags through means other than standard restriction enzyme mediated BioBrick assembly.<sup>12</sup> It is also typically assumed, with reasonable expectations, that the tags minimally perturb the properties of the parent part and therefore do little to fundamentally change the designed property or independence of the parent part itself.

In this manuscript we provide an experimentally validated example demonstrating how the relatively small modification of a commonly used part encoding the transcriptional repressor *cI* from phage lambda<sup>13</sup> creates a novel function whose functional expression is dependent on the genetic context in which the

Received: October 26, 2012

Published: January 4, 2013

part is used. Specifically, we characterize the contextually dependent appearance of a constitutive promoter element in a commonly used BioBrick (BBa\_C0051), which encodes the *cI* repressor from phage lambda,<sup>13</sup> the 11 amino acid LVA proteolytic degradation tag,<sup>14</sup> a BioBrick standard double-TAA stop codon, a “hidden” barcode sequence,<sup>15</sup> and part of the RFC10 SpeI-XbaI BioBrick<sup>12</sup> scar. We call this novel promoter pKAT. We compare the contextual activity of pKAT to that of the reference promoter part BBa\_J23101<sup>16</sup> and present evidence suggesting that the previously uncharacterized pKAT activity may explain unexpected behavior of characterized devices in which BBa\_C0051 has been used.

## RESULTS AND DISCUSSION

**Discovery of a Promoter Element in BBa\_C0051.** The discovery reported in this manuscript occurred during the construction of a device designed by the 2010 iGEM team at the University of California, Davis. Briefly, a polycistron consisting of BioBrick BBa\_C0051 cloned immediately upstream of BBa\_E1010 (Red Fluorescent Protein)<sup>17</sup> and BBa\_F1610 (*luxI*, AHL autoinducer) in the standard cloning plasmid pSB1A2 (Figure 1) resulted in visible pigment

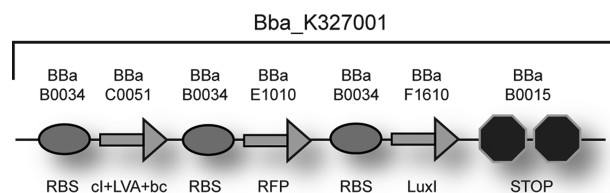


**Figure 1.** A BioBrick composite part: BBa\_K327001. The BioBrick compatible polycistron, BBa\_K327001, containing the phage lambda *cI* repressor (BBa\_C0051), an engineered variant of a red fluorescent protein (BBa\_E1010), and an AHL autoinducer (BBa\_F1610). BBa\_K327001 was constructed using the BioBrick RFC10 assembly standard.<sup>12</sup> In the diagram, ovals represent ribosome binding sites (BBa\_B0034), arrows represent protein coding regions, and the two octagons represent a double transcriptional terminator (BBa\_B0015).

production in *Escherichia coli* DH5 $\alpha$  colonies. This initial construct is named BBa\_K327001. The production of Red Fluorescent Protein (RFP) from BBa\_K327001 was unexpected as BBa\_K327001 lacks any known promoter upstream of either BBa\_C0051 or BBa\_E1010 and plasmid pSB1A2 contains a transcriptional terminator five base pairs upstream of the RFC10 BioBrick standard assembly prefix.<sup>12</sup> Additionally, given the location of the *luxI* gene in context of RFP, there is little reason to believe that BBa\_F1610 plays a role in RFP expression. The regions of BBa\_K327001 encoding the *cI* and RFP proteins were sequenced using Sanger sequencing<sup>18</sup> to verify the nucleotide composition (oligonucleotide primers used for sequencing are listed in Supplementary Table 2). Sanger sequencing confirmed that the construct was correctly built. However, the sequencing also led to the discovery (at least for the authors) that the DNA sequence of BBa\_C0051, between the double-TAA stop codon and the suffix (a region of DNA used in standard assembly encoding recognition sites for endonucleases), contained a “hidden” barcode sequence. Wiki pages describing barcoded BioBrick parts in the Parts Registry now include an explicit warning to users that a barcode is encoded in the part and a hyperlink to a web page describing the barcode program. Users should nevertheless be aware that as of January 1, 2013, the “get sequence” function on a

barcoded part’s wiki page does not yet retrieve the complete barcoded sequence. This task can, however, be accomplished manually by downloading and reading the original DNA sequence data.

The barcode sequence itself consists of 25 nucleotide base pairs (5′-CNCTGATAGTGCTAGTGTAGATCNC-3′) where the identity of nucleotides at positions 2 and 24 (underlined N’s) depend on the name of the barcoded part as calculated by the following formula:  $R = (\text{sum of the digits in the part number}) \bmod 4$ . If  $R$  is 0, then  $N = A$ ; 1, then  $N = C$ ; 2, then  $N = G$ ; 3, then  $N = T$ . These sequences were added to 50 basic parts in the Parts Registry in response to human practice concerns regarding the environmental spread of BioBrick parts.<sup>19</sup> Additional information regarding this short-lived program can be found at the following webpages: <http://partsregistry.org/Help:Barcodes><sup>20</sup> and <http://www.openwetware.org/wiki/Barcodes>.<sup>15</sup> In theory, barcoding allows simple PCR, hybridization, or DNA sequencing methods to identify the presence of BioBricks in any uncharacterized biological sample.

An *in silico* scan for putative  $\sigma^{70}$  promoters encoded within the sequence of BBa\_K327001 was conducted using Delila Tools<sup>21</sup> and other promoter finding tools noted later. No obvious, canonical promoters were found. Delila Tools did reveal a number of possible  $\sigma^{70}$  binding sites above a significance cutoff score of 1.0 within BBa\_C0051. These sites appear throughout the sequence, with a medium-scoring cluster (five sites above 3.9 bits) of possible sites appearing near base 229, and another medium-scoring site (5.9 bits) near base 184. However, since none of these sites were considered high-likelihood candidates we decided to empirically determine the location of the active promoter.

**Determining the Location of the Active Promoter.** To verify BBa\_C0051 as the source of pKAT activity, we cloned BBa\_C0051 into the promoter screening plasmid BBa\_J61002 to create composite part BBa\_K611061. In this plasmid, the standard BioBrick RFC10<sup>12</sup> restriction sites have been shuffled to facilitate the insertion of promoter sequences directly upstream of the genes encoding RFP. Promoter BBa\_J23101, proposed as a standard for constitutive promoters by Kelly et al.,<sup>16</sup> was also cloned into BBa\_J61002 as a positive control (BBa\_J162003). As described below, background subtracted fluorescence levels for several constructs (i.e., BBa\_K611074–9) were between 2% and 3% of those reported for BBa\_J23101. These clones served ostensibly as promoter negative controls, confirming that the observed promoter activity was not inherent in the BBa\_J61002 backbone but was rather a function of the sequences we inserted in the cloning site. As expected, insertion of BBa\_C0051 and BBa\_J23101 into the promoter screening plasmid induced visible pigment production (Supplementary Figure 1). We concluded that the promoter element in BBa\_K327001 originated somewhere within the sequence of BBa\_C0051.

All promoter strength hereafter is reported in relative promoter units (RPU) as described by Kelly et al.<sup>16</sup> unless otherwise noted. The “whole cell qPCR” method described in ref 22 and detailed in the Supplementary Text and Method was also used to rule out the unlikely possibility that differences in the reported RPU might be attributed to differences in plasmid copy number.

In order to restrict the search region, 5′ truncations of BBa\_C0051 were created. PCR primers (Supplementary Table 2) were designed to amplify five serially truncated fragments of

BBa\_C0051 (5' truncation lengths of 3, 110, 260, 431, and 560 bp) (Figure 2a). These truncation products were individually

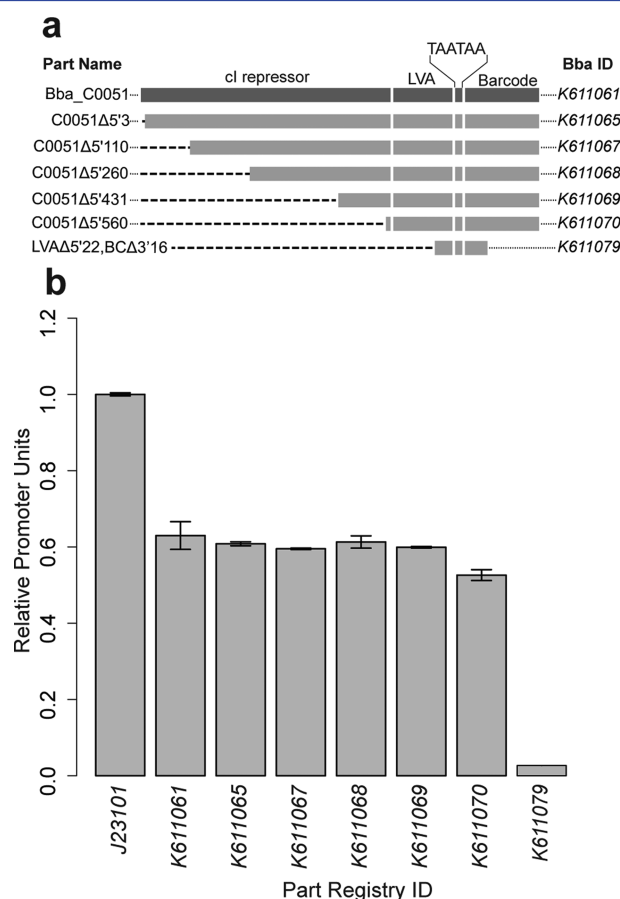


**Figure 2.** Relative promoter units of BBa\_C0051 5' truncations. BBa\_C0051 truncations were constructed by using PCR to amplify out equivalent sections of BBa\_C0051. (a) Each truncation was cloned into the promoter screening plasmid (BBa\_J61002) and given a new Bba ID (far right). Each truncation retained the full LVA-protolytic degradation tag, double TAA stop codon, barcode, and SpeI-XbaI scar. (b) Background subtracted relative fluorescence of each truncation is reported in relative promoter units (RPU) to the reference promoter, BBa\_J23101, as described by Kelly et al.<sup>16</sup> Error bars represent  $\pm 1$  SD from the mean. BBa\_K611079 is a negative control.

cloned into the promoter screening plasmid BBa\_J61002 to test whether or not a promoter element existed within each product. It is important to note that for convenience the truncations reported herein lack the NotI and XbaI restriction sites found in the BioBrick RFC10 Assembly Standard prefix.<sup>12</sup> This creates a difference of 17 base pairs between BBa\_K611065 (BBa\_C0051Δ5'3) and the original BBa\_K611061 construct. The fluorescence and optical density of each construct was measured as described in Methods. In each experimental run, BBa\_J162003 was included as an internal positive control. All truncations showed RPUs ranging from 0.53 to 0.61 RPU of the standard reference promoter BBa\_J23101 (Figure 2b). This experiment determined that pKAT must be encoded in the 3' most 254 bp of BBa\_C0051.

To more specifically identify the region encoding pKAT, we decided to further investigate the 3' end of BBa\_K611070. DNA oligonucleotide PCR primers (Supplementary Table 2) were designed to construct 8 different truncated versions of BBa\_K611070 (Figure 3a). This allowed us to assess which

portions of the last 190 base pairs of the cI coding region, LVA proteolytic degradation tag, the double-TAA stop codon, and the barcode sequence were potentially involved in RNA polymerase holoenzyme recruitment. In addition to the constructs above, we also placed the barcode sequence alone upstream of RFP (BBa\_K611071). Measurements of RPUs (Figure 3b) showed that BBa\_K611071 activity decreases to near (though not completely) baseline activity (0.11 RPU). Identical tests with the 190 bp cI + LVA truncations BBa\_K611072 and BBa\_K611073 showed activity of 0.44 RPU and 0.51 RPU, respectively. When any portion of the Barcode was truncated (BBa\_K611074 and BBa\_K611075), all activity was lost. As expected, constructs combining barcode and 190 bp cI + LVA truncations (BBa\_K611076, BBa\_K611077, BBa\_K611078, and BBa\_K611079) had little discernible activity.

The initial round of molecular cloning and characterization of the truncations described above resulted in several constructs in which the first thymine of the SpeI-XbaI scar was deleted between BBa\_C0051 and ribosome binding site of BBa\_E1010. Figure 3b shows data for a representative construct, LVAΔ5'11,Δ+1 (BBa\_K611084). This mutant showed 52% of the activity of its T-containing counterpart (BBa\_K611072). In this specific context, this data implicates the role of one of the most common RFC10-based BioBrick sequence elements,<sup>12</sup> the SpeI-XbaI scar (TACTAGA), as a contributor to the pKAT element.

By convention, protein coding BioBrick parts are recommended to end with a double-TAA stop codon (TAATAA). The nucleotide composition of the double-TAA stop codon and its position in the promoter containing sequences identified in Figure 3 resemble other known functionally important AT-rich promoter elements such as bacterial Pribnow boxes<sup>23,24</sup> and eukaryotic and archaeal TATA box. We therefore decided to test whether the double-TAA stop codon also contributes to the pKAT element when it directly precedes a barcode. Site directed mutagenesis was performed as described in Methods to construct a TGATAA double stop codon mutant. The resulting mutant had an activity of 0.35 RPU, nearly 0.28 RPU (or 55%) less than the construct containing the double-TAA stop codon (Figure 3b). A summary of all relevant parts constructed in this section can be found in Supplementary Table 1.

### Experimentally Determining the Transcript Start Site.

To determine the location of the transcriptional start site (TSS) within the BBa\_K327001 construct, 5'-RACE experiments were conducted as described in Methods. Two independent colonies of BBa\_K327001 were tested along with an endogenously RFP-expressing construct containing BBa\_J23101 in BBa\_J61002 (BBa\_J162003, positive control), and wild-type *Escherichia coli* DH5α cells (negative control). Sanger sequencing of the amplified cDNA revealed identical sequence following the polyA tail for the experimental duplicates and the positive RFP control, while no discernible signal was found in the DH5α negative control (Supplementary Figure 3). Thus, the location of the transcriptional start sites for the pKAT (in BBa\_K327001) and BBa\_J23101 (in BBa\_J61002) promoters appear to be identical. Specifically, the sequence data revealed that the TSS for both pKAT and BBa\_J23101 are located at the first thymine of the XbaI-SpeI scar upstream of BBa\_B0034, which is consistent with the observed functional role of this thymine suggested during the characterization of the LVAΔ5'11,Δ+1 (BBa\_K611084)

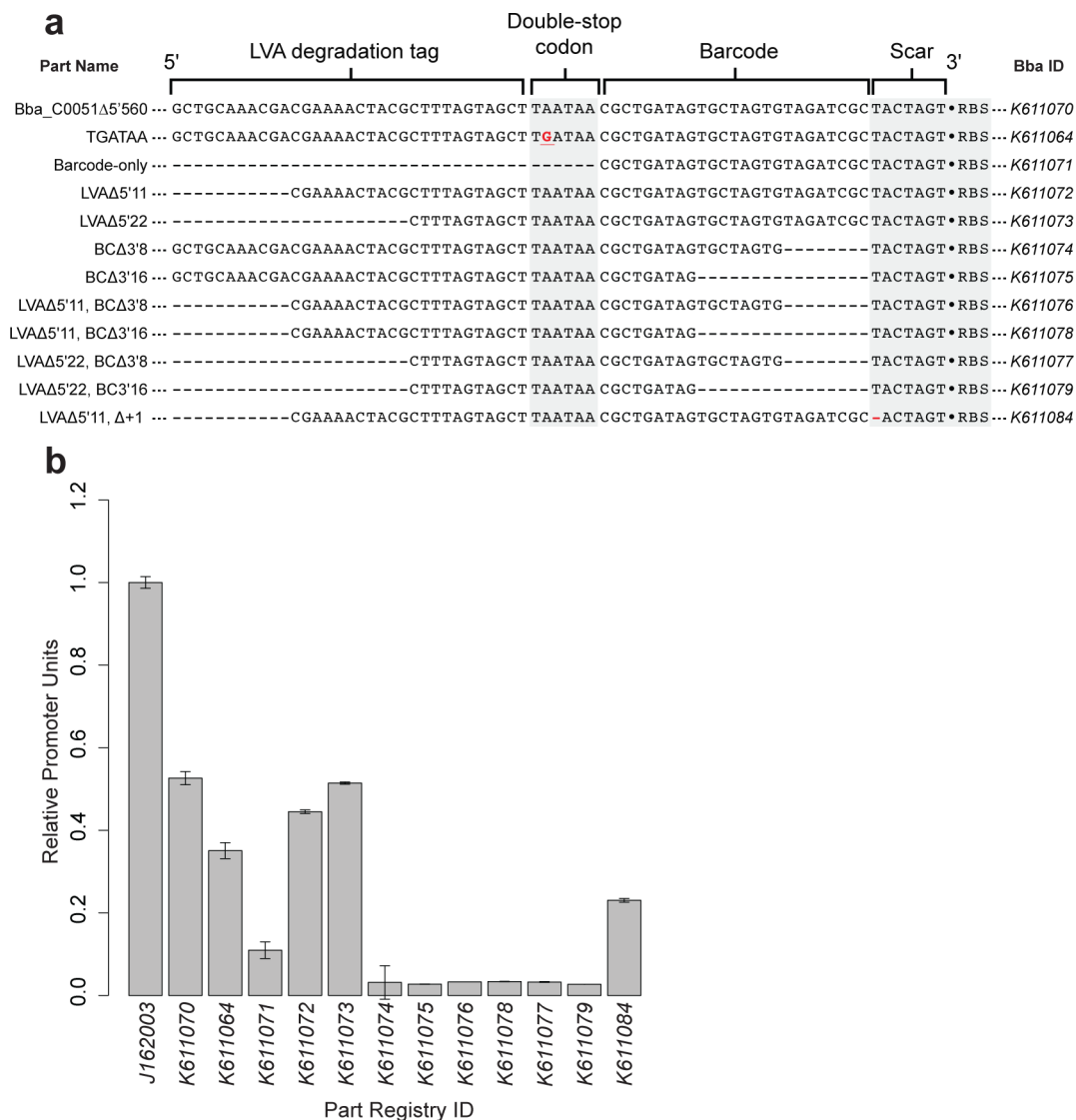


**Figure 3.** Relative promoter units of LVA and barcode truncations from BBa\_K611070. DNA oligonucleotides were designed to create truncations of BBa\_K611070. (a) Each truncation was annealed and ligated into the promoter screening plasmid BBa\_J61002 and given a new BBa ID (far right). A dash denotes a deletion, and single point mutations are highlighted in red. (b) Background subtracted relative fluorescence is reported as RPUs to the reference promoter BBa\_J23101 as described by Kelly et al.<sup>16</sup> Error bars represent  $\pm 1$  SD from the mean.

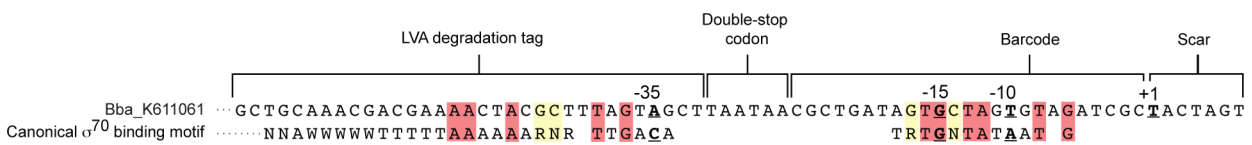


**Figure 4.** Alignment of the putative pKAT promoter with a canonical  $\sigma^{70}$  promoter. A pairwise alignment of the experimentally determined pKAT region to a canonical  $\sigma^{70}$  promoter. The  $-35$ ,  $-15$ ,  $-10$ , and  $+1$  sites are annotated. The corresponding bases are underlined and rendered bold. Red highlighting indicates identity between nucleotides, the canonical promoter, and pKAT, and yellow highlighting indicates partial conservation. A, C, G, and T correspond to the common nucleotide bases, R encodes A or G, N encodes A or C or G or T, and W encodes A or T. The functional subelements of pKAT are indicated above the sequence.

construct. If the promoter adheres to the canonical model for sigma factor and RNA polymerase (RNAP) binding in *Escherichia coli*, key promoter elements are likely to be found in the following two regions:  $-7$  to  $-15$  bp and  $-30$  to  $-35$  bp with respect to the TSS. In the BBa\_K327001 construct these functional promoter elements are found spanning the barcode ( $-7$  to  $-15$ ), the double-TAA stop codon, and the LVA tag ( $-30$  to  $-35$ ).

In total, these genetic analyses demonstrate that the sequences encoding the pKAT element can be confined within all elements in BBa\_611073 and the SpeI-XbaI scar. While each of the components within BBa\_611073 contribute to the promoter element, the transcriptional activity can be simply eliminated by removing the barcode. A version of BBa\_C0051 lacking the barcode was therefore created and cloned into the promoter screening plasmid BBa\_J61002 to create BBa\_K611066. As expected, BBa\_K611066 showed no



discernible RFP expression (Figure 3b). A corresponding version of BBa\_C0051 lacking the original barcode has been submitted to the Parts Registry in standard BioBrick format and has been assigned the name BBa\_K327018.

**Informatic Analysis of the pKAT.** With the location of pKAT narrowed to 49 bps we sought to further investigate this sequence for any evidence of canonical promoter elements. The sequence of BBa\_C0051 encompassing the LVA tag, double-TAA stop codon, and barcode was aligned to the general *Escherichia coli*  $\sigma^{70}$  promoter motif 5'-TTGA-CANNNNNNNNNNNNNNNNTRTGNTATAATNGNNNN-3' (underlined elements indicate -10 and -35 elements, italic font indicates the extended -10 element)<sup>25,26</sup> using the EMBOSS Stretcher pairwise sequence alignment tool (Gap penalty: 16, Extend penalty: 4).<sup>27</sup> The alignment reveals low sequence identity in the regions of the canonical -10 (TATAAT - 33%) and -35 (TTGACA - 33%) motifs (Figure 4). Nevertheless, the two conserved bases within both the putative -10 region and the putative -35 region have been found to be most the most critical nucleotides in the DNA to  $\sigma^{70}$  holoenzyme interaction<sup>28,29</sup> and these were conserved in the alignment. Additionally, base pairs 13 to 16 upstream of the experimentally determined TSS show 100% identity to the canonical promoter. This region corresponds well to the previously characterized -15 element (TGNT) described in weak *Escherichia coli*  $\sigma^{70}$  promoters with degenerate -10 and -35 elements.<sup>25,26,30</sup> Finally, while the double-TAA stop codon does not align with any of the canonical regions in the  $\sigma^{70}$  motif, studies on certain *E. coli* promoters have shown that the size and content of the spacer between the -10 and -35 elements have an affect on promoter function and strength due to favorable and unfavorable DNA mechanics associated with holoenzyme binding.<sup>31-33</sup>

The model for the promoter suggested by the alignment is consistent with the LVA tag/double-TAA stop codon/barcode truncation data. Removal of 8 base pairs from the 3' end of the barcode creates a shift in reference to the TSS so that the -10, -15, and -35 elements no longer have the correct conformation for  $\sigma^{70}$  binding. Meanwhile, the removal of 16 base pairs from the 3' end of the barcode would completely truncate both the -10 and -15 elements, which are essential DNA- $\sigma^{70}$  binding nucleotides. On the other hand, truncating the first 22 base pairs off the 5' end of the LVA tag has no effect, which is also consistent with the model.

The sum of genetic and informatic analyses presented thus far support the conclusion that each of the four functional elements (an LVA proteolytic degradation tag, a double-TAA stop codon, a barcode, and a SpeI-XbaI scar) encoded within a 49 bp composite sequence can function as a constitutive promoter in *Escherichia coli*. The most essential element appears to be the barcode. However changes within the TAATAA region as well as the eight 3' most bases of the LVA tag also reduce promoter strength significantly. This observation is highlighted in another common protein coding BioBrick part, BBa\_E1010, which contains a double TAATAA stop codon and barcode but lacks the LVA proteolytic degradation tag. Unsurprisingly, when tested in BBa\_J61002 this construct fluoresced at levels similar to BBa\_K611071 (Supplementary Figure 1). While not explicitly tested, an analysis of the alignment in Figure 4 also reveals that the variable second and 24th base in the barcode fall outside the canonically important positions. This suggests that any part containing the LVA/TAATAA/Barcode/Scar sequence, regardless of which version

of the barcode is incorporated, may also show transcription of adjacent downstream genes.

**Conditional Characterization of the Promoter.** After determining the minimal sequence for defining pKAT, we sought to further characterize the conditional activity of pKAT relative to the standard promoter BBa\_J23101.<sup>16</sup> Promoter strength can vary significantly depending on genetic and environmental context and therefore even efforts to define promoter strength relative to a specific standard<sup>16</sup> require that the environmental and genetic conditions be rigorously defined. Since condition-space is impossibly large, we tested the promoter elements within BBa\_J23101, BBa\_K611061, BBa\_K611064, BBa\_K611071, and BBa\_K611074 in standard growth conditions (37 °C in LB broth) and in response to three environmental perturbations of specific interest to our laboratory, perturbed temperature (33 and 42 °C) and 0.6 M NaCl (1.2 Osm) induced ionic/osmotic stress. These three stress conditions are known to induce differential activity of alternate sigma factors, such as the stress related sigma factor  $\sigma^{32}$  (RpoH),<sup>34-36</sup> and therefore together test the hypothesis that a change in sigma factor activity may reveal conditional differences between BBa\_J23101 and pKAT.

While all tested promoters showed changes in promoter strength during stress relative to that shown in standard conditions (Figure 5a), the RPU of pKAT and pKAT-derived promoters relative to that of BBa\_J23101 remain constant across the tested conditions (Figure 5b). This result implies that (at least under these specific operational conditions) the mechanisms of transcriptional initiation of pKAT and BBa\_J23101 may be identical.

**In Silico Detection of Putative Promoters.** In order to evaluate the power of various *in silico* methods for detecting pKAT or pKAT-like promoters, we examined the DNA sequence composed of 200 base pairs flanking either side of the barcode (for a 425 bp total sequence) in BBa\_K327001 with the following algorithms: BPROM (<http://www.softberry.com/berry.phtml>), the neural network-based detection tool NNPP ([http://www.fruitfly.org/seq\\_tools/promoter.html](http://www.fruitfly.org/seq_tools/promoter.html)),<sup>37,38</sup> the Hidden Markov Model-based detection program PPP ([http://bioinformatics.biol.rug.nl/websoftware/ppp/ppp\\_start.php](http://bioinformatics.biol.rug.nl/websoftware/ppp/ppp_start.php)),<sup>39</sup> as well as an online demo ([http://nostradamus.cs.rhul.ac.uk/~leo/sak\\_demo/](http://nostradamus.cs.rhul.ac.uk/~leo/sak_demo/)) of the Sequence Alignment Kernel (SAK) method.<sup>40</sup> As a positive control, we replaced the putative promoter region with the sequence of strong promoter BBa\_J23101 and tested each method on both sequences.

All methods were able to detect the known strong promoter BBa\_J23101. The BPROM utility was unable to detect pKAT, though it detected a putative promoter 34 bases upstream of the experimentally determined TSS. NNPP was unable to detect a promoter in the sequence with default settings. When the scoring threshold was lowered, a weakly scoring putative promoter (score 0.52, with default minimum score 0.80) was detected with a predicted transcriptional start located on the 5'-most nucleotide of the barcode, about 25 bases before the experimentally verified TSS. PPP did not detect any putative promoter. The SAK method found a peak with a scoring probability equal to 0.3 at the pKAT's experimentally determined transcriptional start site while the scoring probability of the positive control promoter equaled 0.6. However, the SAK method also detected putative promoters with probabilities similar to that of the pKAT throughout the search sequence, which were not experimentally detected. This

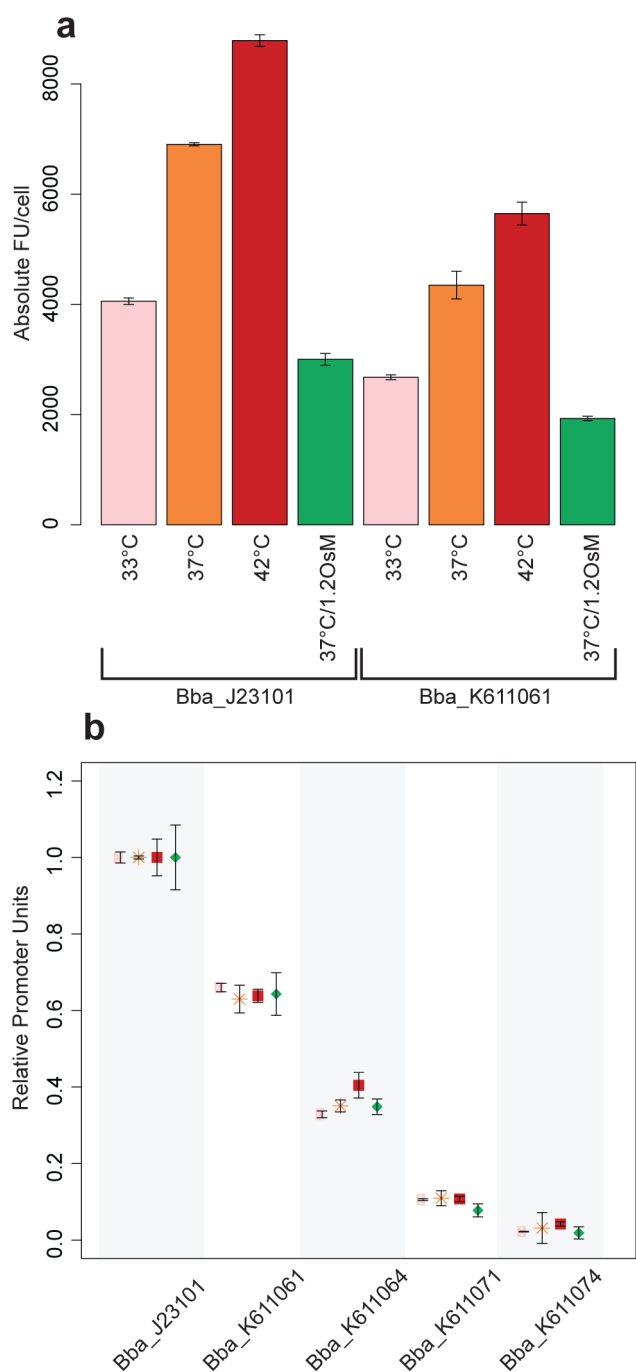


**Figure 5.** Conditional activity of pKAT and Bba\_J23101. (a) Absolute activity of Bba\_J23101 and pKAT (Bba\_K611061) at 33, 37, and 42 °C and standard salinity and as measured at 37 °C at 1.2 OsM. Error bars indicate  $\pm 1$  SD from the mean. These data indicate that in each case promoter strength is dependent on environmental conditions. (b) Activity of pKAT and pKAT truncations relative to that of Bba\_J23101 at each condition listed in panel a. Pink circles indicate growth at 33 °C (standard salinity), orange stars indicate growth at 37 °C (standard salinity), red squares indicate growth at 42 °C (standard salinity), and green diamonds indicate growth at 37 °C (1.2 OsM). Note that while absolute fluorescence per cell differs for each construct, RPU remain constant for each construct in nearly all tested conditions, suggesting that the requirements for transcriptional initiation of both Bba\_J23101 and pKAT are likely identical.

analysis, therefore, leads to the conclusion that existing promoter-finding tools would not have detected the pKAT *a*

*priori* and that they currently lack sufficient predictive power for routine “preventative” screening and identification of high-likelihood promoters in novel genetic constructs.

**Other BioBrick Parts with Similar Motifs.** An analysis of sequences comprising the Parts Registry revealed that 50 basic parts, defined loosely as any part irreducible by any other part, contained “hidden” barcodes (see Methods for details on the precise definition of a basic part and analytical methods). While a modest portion of all basic parts, these 50 bar-coded basic parts are used extensively in composite parts (Figure 6a and

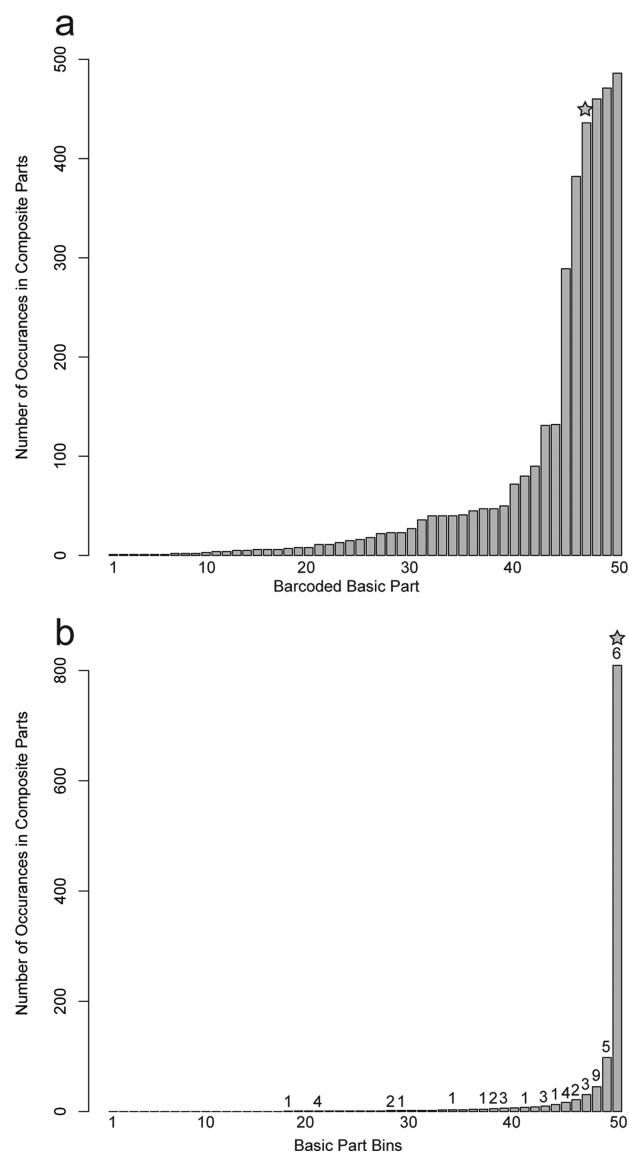


**Figure 6.** Number of basic parts in the Parts Registry containing “hidden” barcodes and their frequency-of-use. (a) Fifty bar-coded basic parts were discovered in the Parts Registry. Each column represents a single bar-coded basic part, and the column-part mapping can be found in Supplementary Table 3. The vertical axis indicates the frequency with which each bar-coded basic part was found in a composite part in the Parts Registry. Part Bba\_C0051 is annotated with a star. (b) The frequency with which all basic parts are found in composite parts. Each bin contains 42 parts, with the exception of bin 1 that contains 79 parts. The average use of parts in each bin is plotted along the vertical axis. Numbers above each bar indicate the number of bar-coded basic parts found in each bin. The bin annotated with the star contains Bba\_C0051.

Supplementary Table 3). These 50 bar-coded basic parts are found to be reused in 27% (2,459) of the total parts in the Parts Registry. Moreover, these bar-coded basic parts had a significantly higher reuse rate than the overall average of basic parts not containing barcodes (Figure 6b).

In addition to barcoded parts, we were interested to identify other BioBricks in the Parts Registry that might contain pKAT or pKAT-like promoters. Since detecting pKAT-like promoters *de novo* proved challenging we conducted a more direct search of the Parts Registry by manually converting the core 49 base pairs determined by our experiments to define the pKAT promoter element, into a position weight matrix (PWM). Weights for nucleotides that occur within the putative  $-10$ ,  $-15$ , and  $-35$  elements of the canonical  $\sigma^{70}$  motif and also the TAATAA double stop codon were set to 1, while nucleotides at all other positions were given equal weight = 0.25 (Figure 4). We then used the Motif Alignment and Search Tool (MAST<sup>41</sup>) from the MEME Suite<sup>42</sup> to search for occurrences of the pKAT motif in the Parts Registry as described in Methods.

We began by gathering a large list of putative promoters by using relaxed positional  $p$ -value (0.01) and  $E$ -value (100) constraints. This search resulted in 83,109 matches of the pKAT motif in 2,543 parts. To filter this preliminary list for “high-confidence” occurrences of pKAT, we ran multiple independent MAST runs, systematically decreasing the positional  $p$ -value constraint by steps of 0.01 each time. A positional  $p$ -value of  $8.73 \times 10^{-16}$  returned motif matches in which bases corresponding to the  $-10$ ,  $-15$ ,  $-35$  elements, and the double stop codon were identical to those in the PWM describing pKAT (2,665 matches spanning 1,696 parts) (Supplementary Table 4). Relaxing the MAST  $p$ -value (greater than  $8.73 \times 10^{-16}$ ) returns 1,245 additional matches to the pKAT motif (encoded in 1,116 parts) in which some of the  $-10$ ,  $-15$ ,  $-35$  elements and double stop codon differed from those in the PWM. All of these motif occurrences (up to a  $p$ -value of  $1.10 \times 10^{-6}$ ) consist of barcodes that are not in proximity of an LVA-tag. Despite the variability at the 5'-end of these putative pKAT promoters (a region shown to be important for maximal activity), we nevertheless consider these potentially important, because our barcode-only constructs (BBa\_K611071) suggest that low-level transcription from pKAT-like promoters may still occur. A detailed list of these occurrences can be found in Supplementary Table 5.

Lastly, we asked how many of the putative pKAT promoters discovered in the Registry might be expected to lead to unwanted transcription of downstream elements based on their genetic context in composite parts. This was accomplished by adding 24–30 additional bases to the 3'-end of the pKAT PWM to model a SpeI-XbaI scar (PWM weights = 1 for nucleotides in scar), a ribosome binding site (PWM weights = 0.25 for each nucleotide in the RBS spacer), a second SpeI-XbaI scar (PWM weights = 1 for nucleotides in scar) and an ATG start codon (PWM weights = 1). From this MAST search, we report that 439 parts ( $\sim 5.2\%$  of the Parts Registry) have at least one “high-confidence” instance of a predicted pKAT-like promoter directly upstream of an RBS and ATG start site. These parts are listed in Supplementary Table 6.

**Summary and Conclusion.** A foundational tenet of synthetic biology proposes that well-characterized and composable parts may be used to predictably build complex modular systems. The notion that each biological part be functionally independent, regardless of context (e.g., a promoter retains the same quantifiable function in different

constructs), follows naturally from this hypothesis. The pKAT promoter discovered in this study is localized to a region of BBa\_C0051 encoding an LVA proteolytic degradation tag, a double-TAA stop codon, a genetic barcode, and an RFC10 BioBrick scar. The promoter element arises from the specific combination of otherwise independent functional parts demonstrating the functional plasticity of DNA and violating the notion of contextual independence proposed above. Our results argue for the development of tools (computational and experimental) capable of predicting and measuring the emergence of similar phenomena on a system-wide scale. Withal, bioengineers may ultimately learn to better utilize DNA's plasticity to increase the density of functional units in genetic circuits.

## METHODS

**Molecular Assembly.** Unless otherwise stated, assembly of all molecular components were accomplished by standard assembly as specified by RFC10.<sup>12</sup> Truncation products were built by PCR amplifying abbreviated segments of the BBa\_K611061 construct with 5' oligonucleotides containing DNA sequences encoding the standard RFC10 BioBrick prefix.

**Site Directed Mutagenesis.** Site directed mutagenesis of the double stop codon (TAATAA) was performed as described by Stratagene. Briefly, BBa\_K611061 was cultured and miniprep from *Escherichia coli* DH5 $\alpha$  cells using a PureJet Miniprep Kit (Invitrogen, Carlsbad CA). A 50  $\mu$ L reaction mixture consisting of 5  $\mu$ L of 10X Pfu Turbo Buffer, 3.0  $\mu$ L of 2.5 mM Mutation Primer Mix (described previously), 1  $\mu$ L of 10 mM dNTPs, 1  $\mu$ L of Pfu Turbo, 1  $\mu$ L of miniprep construct, and 39  $\mu$ L of Milli-Q H<sub>2</sub>O was mixed in a thin-walled 200  $\mu$ L PCR tube. Tubes were placed in a Dyad Peltier Thermocycler (Bio-Rad, Hercules CA), and the following PCR protocol was run: (1) 95 °C for 2 min; (2) 95 °C for 30 s; (3) 55 °C for 1 min; (4) 68 °C for 4 min; (5) repeat steps 2, 3, and 4, 17 times; (6) 68 °C for 10 min. Once the reaction was complete, 1  $\mu$ L of DpnI (New England Biolabs, Ipswich MA) was added directly into the PCR cocktail and digested at 37C for 2.5 h. Five microliters of digestion product was directly transformed into 50  $\mu$ L of “ultra-competent” *E. coli* DH5 $\alpha$  cells as described by Sambrook and Russell.<sup>43</sup> Colonies were screened and sequenced using universal forward (VF2 - BBa\_G00100) and reverse (VR - BBa\_G00101) primers to validate mutation(s).

**Determining Transcript Start Site Using 5'-RACE.** 5'-RACE was performed as described by Griffiths.<sup>44</sup> RNA was extracted from *Escherichia coli* DH5 $\alpha$  cells harboring the BBa\_K327001 construct using a RNeasy Mini Kit (Qiagen, Germany). Reverse transcription was performed on the following mixture: 14  $\mu$ L of sterile Milli-Q water, 2  $\mu$ L of 10  $\mu$ M Reverse Transcription Primer, 10  $\mu$ L of purified RNA, and 2  $\mu$ L of RNase-free 10 mM dNTP. The mixture was incubated at 65 °C for 5 min and subsequently placed on ice for 1 min. After cooling the sample was centrifuged for 20 s at 11,000g in an Eppendorf 5424 Centrifuge (Germany). Eight microliters of SX first strand buffer, 2  $\mu$ L of 0.1 M DTT, and 2  $\mu$ L of Superscript III RT (Invitrogen, Carlsbad CA) were added to the mixture. This was incubated at 50 °C for 1 h and then immediately stored at  $-20$  °C for storage. For analysis, reverse transcription products were thawed from  $-20$  °C, incubated at 100 °C for 2 min, and then immediately placed on ice. RNA that remained after reverse transcription was removed by the addition of 1.5  $\mu$ L of RNase A and incubated for 10 min at 37



°C. First strand DNA was then purified using a Nucleic Acid and Protein Purification Kit (Macherey-Nagel, Germany).

Poly-A tails were added to the first strand DNA by mixing 7  $\mu\text{L}$  of Nuclease Free Water (Ambion, USA), 7  $\mu\text{L}$  of purified first strand DNA, 2  $\mu\text{L}$  of NEB Buffer 4, 2  $\mu\text{L}$  of  $\text{CoCl}_2$ , 1  $\mu\text{L}$  of 2 mM dATP, and 1  $\mu\text{L}$  of Terminal Transferase (New England Biolabs, Ipswich MA) and incubating at 37 °C for 30 min. Amplification of the poly-A tailed first strand DNA was accomplished through PCR with a reaction recipe of 35.4  $\mu\text{L}$  of Nuclease Free Water, 5  $\mu\text{L}$  of 10X Buffer, 1.2  $\mu\text{L}$  of dNTP, 0.4  $\mu\text{L}$  of Taq polymerase (Qiagen, Germany), 2  $\mu\text{L}$  of poly-A tailed first strand DNA, 3  $\mu\text{L}$  of 10  $\mu\text{M}$  PolyT Primer, and 3  $\mu\text{L}$  of 10  $\mu\text{M}$  Reverse Transcription Primer. Reactions were amplified in a Dyad Peltier Thermocycler (Bio-Rad, Hercules CA) using the following PCR protocol: (1) 7 min at 98 °C; (2) 45 s at 98 °C; (3) 1 min at 48 °C; (4) 30 s at 72 °C; (5) repeat steps 2, 3, and 4, 26 times; (6) 5 min at 72 °C. PCR amplification products were cleaned using a Nucleic Acid and Protein Purification Kit and 5  $\mu\text{L}$  of product was run on a 2% agarose gel at 100 V to verify synthesis (Supplementary Figure 2).

A second amplification reaction was performed using the same reaction recipe above but by replacing the Reverse\_Transcription\_Primer with the E1010\_Outside\_Primer. The thermocycler program was identical to that above with the exception of an increasing the annealing temperature in step 3 to 54 °C. PCR amplification products were again cleaned using a Nucleic Acid and Protein Purification Kit, and 5  $\mu\text{L}$  of product was again run on a 2% agarose gel at 100 V to verify synthesis. PCR products from the second amplification were blunt end cloned into the *StuI* site of the high copy backbone plasmid pNBK07 (Supplementary Figure 4 and Supplementary Sequence 1) for sequencing. pNBK07 was originally obtained from N. Baliga (Institute for Systems Biology, Seattle, WA) and has been previously used to create targeted genomic insertions and deletions in *Halobacterium salinarum* NRC-1.<sup>45,46</sup> Sanger sequencing was performed at the UC Davis DNA Sequencing Facility using the pNBK07\_F primer (Supplementary Table 2) with the Applied Biosystems BigDye Terminator Version 3.1 Cycle Sequencing chemistry on an Applied Biosystems 3730 Capillary Electrophoresis Genetic Analyzer (Applied Biosystems, Foster City CA). Sequences were analyzed using the software 4Peaks.<sup>47</sup>

#### Fluorescence and Optical Density Measurements.

Fluorescence testing was performed using a Tecan Infinite M200 (Tecan, Switzerland) plate reader with Greiner 96-well flat bottom clear polystyrene plates (product no. 3595) (Greiner, Austria). Before plating, a starter culture of 5 mL of LB with 100  $\mu\text{g}/\text{mL}$  carbenicillin was inoculated from freezer stock and grown to saturation over  $\sim 14$  h. Using the starter culture as inoculum, an additional 5 mL preculture was grown, in LB with 100  $\mu\text{g}/\text{mL}$  carbenicillin, for  $\sim 3$  h to an optical density ranging from 0.5 to 0.7 as measured at 600 nm ( $\text{OD}_{600}$ ). The cells from this preculture were then used to inoculate 200  $\mu\text{L}$  of LB media with 100  $\mu\text{g}/\text{mL}$  carbenicillin to yield a starting optical density of  $\text{OD}_{600} \approx 0.01$ . Cells were grown at 37 °C (fluctuation between 36.4 and 37.5 °C was allowed) with orbital shaking at an amplitude of 2.5 mm. The growth program consisted of 80, 10 min cycles in which fluorescence and  $\text{OD}_{700}$  was measured after each cycle. Fluorescence was measured in each sample well from the top of the sample through a clear cover in a 3  $\times$  3 filled square pattern.

For measurements involving RFP, optical density was measured at 700 nm ( $\text{OD}_{700}$ ).  $\text{OD}_{700}$  was measured using 25 flashes with a settle time of 0 ms. The fluorescence excitation wavelength was 588 nm and emission was read at 615 nm. Individual measurements were obtained over a 3  $\times$  3 filled square pattern using 25 flashes, a 20  $\mu\text{s}$  integration time, and 50% detector gain. Lag and settle time were both 0  $\mu\text{s}$ .

**Motif Search Using MAST.** A FASTA file containing a catalog of parts in the Parts Registry was downloaded January 24, 2012 from [http://partsregistry.org/fasta/parts/All\\_Parts](http://partsregistry.org/fasta/parts/All_Parts). Parts less than the 42 bp core promoter sequence were trimmed from the FASTA file using the MATLAB Bioinformatics Toolkit as they would be too short to contain viable pKAT promoters. A MAST input file was manually created to represent background 51% A/T 49% GC frequencies and our consensus promoter motif. MAST queries were constrained with *p*-value and *E*-value such that only an exact match of the position weight matrix was returned. All MAST queries were analyzed using the MEME Software Suite.<sup>41</sup>

**Discovery of Parts Containing Hidden Barcodes in Parts Registry.** First, all short parts (designated by an associated sequence fewer than 10 nt in length) and all deprecated parts were trimmed from the FASTA file using the MATLAB Bioinformatics Toolkit; small parts (e.g., some promoters) were manually returned to the main part list. Second, a manually curated list of auxiliary parts, defined as coding elements that could be used to add auxiliary functions to other parts (e.g., epitope tags, degradation tags, etc.) was created. A complete list of these auxiliary parts is available in Supplementary Table 7. Third, an all-versus-all pairwise string matching calculation was conducted for all nonauxiliary verified parts. In every case where a “part’s” whole reported sequence was discovered within the sequence of another “part’s” reported sequence, the part with shorter sequence was considered to be a component of the longer sequence part (a complete list of the components of each part is available in Supplementary File 1). Parts that had no nonauxiliary component parts (or were members of a short, manually inspected list, available in Supplementary Table 8) were deemed basic; all remaining nonauxiliary parts were composite.

## ■ ASSOCIATED CONTENT

### 📄 Supporting Information

This material is available free of charge via the Internet at <http://pubs.acs.org>.

## ■ AUTHOR INFORMATION

### Corresponding Author

\*E-mail: [mtfacciotti@ucdavis.edu](mailto:mtfacciotti@ucdavis.edu).

### Author Contributions

<sup>†</sup>These authors contributed equally to this work. K.O. and T.F. conceived the study, collected and interpreted data, and participated in the preparation of the manuscript; A.I.Y., P.S., D.J.L., H.S., J.L., A.N., P.S., and J.T. collected and interpreted data and participated in the preparation of the manuscript; I.T. participated in the preparation of the manuscript; M.T.F. conceived the study, interpreted the data, and participated in the preparation of the manuscript.

### Notes

The authors declare no competing financial interest.



## ACKNOWLEDGMENTS

Funding was provided through M.T.F.'s start-up fund and discretionary contributions of the UC Davis Genome Center and UC Davis College of Engineering. Additional funding through private donations were received from Mr. Roger Salquist, Mr. Chad Schwartz, Dr. Daniel Facciotti and Mrs. Christine Facciotti, Dr. Wayne Fenton Jr. and Mrs. Jeanne Joe-Fenton, Mr. Wayne Fenton and Mrs. Suzy Fenton, and Mr. Alex Novichenock. Summer salary for I.T. was provided by NSF award 1146926.

## REFERENCES

- (1) Bennett, G. *What is a Part?*, [http://www.biofab.org/sites/default/files/HPIP\\_DraftReport\\_Parts\\_1.0.pdf](http://www.biofab.org/sites/default/files/HPIP_DraftReport_Parts_1.0.pdf).
- (2) Knight, T. (2003) *Idempotent Vector Design for Standard Assembly of Biobricks*, <http://hdl.handle.net/1721.1/21168>.
- (3) Anderson, J. C., Dueber, J. E., Leguia, M., Wu, G. C., Goler, J. A., Arkin, A. P., and Keasling, J. D. (2010) BglBricks: A flexible standard for biological part assembly. *J. Biol. Eng.* 4, 1.
- (4) Brown, J. (2007) The iGEM competition: building with biology. *IET Synth. Biol.* 1, 3–6.
- (5) Tabor, J. J., Bayer, T. S., Simpson, Z. B., Levy, M., and Ellington, A. D. (2008) Engineering stochasticity in gene expression. *Mol. Biosyst.* 4, 754–761.
- (6) Tabor, J. J., Salis, H. M., Simpson, Z. B., Chevalier, A. A., Levskaya, A., Marcotte, E. M., Voigt, C. A., and Ellington, A. D. (2009) A synthetic genetic edge detection program. *Cell* 137, 1272–1281.
- (7) Tamsir, A., Tabor, J. J., and Voigt, C. A. (2010) Robust multicellular computing using genetically encoded NOR gates and chemical 'wires'. *Nature* 469, 212–215.
- (8) Lou, C., Liu, X., Ni, M., Huang, Y., Huang, Q., Huang, L., Jiang, L., Lu, D., Wang, M., Liu, C., Chen, D., Chen, C., Chen, X., Yang, L., Ma, H., Chen, J., and Ouyang, Q. (2010) Synthesizing a novel genetic sequential logic circuit: a push-on push-off switch. *Mol. Syst. Biol.* 6, 350.
- (9) Bonnet, J., Subsoontorn, P., and Endy, D. (2012) Rewritable digital data storage in live cells via engineered control of recombination directionality. *Proc. Natl. Acad. Sci. U.S.A.* 109, 8884–8889.
- (10) Dragosits, M., Nicklas, D., and Tagkopoulos, I. (2012) A synthetic biology approach to self-regulatory recombinant protein production in *Escherichia coli*. *J. Biol. Eng.* 6, 2.
- (11) Peccoud, J., Blauvelt, M. F., Cai, Y., Cooper, K. L., Crasta, O., DeLalla, E. C., Evans, C., Folkerts, O., Lyons, B. M., Mane, S. P., Shelton, R., Sweede, M. A., and Waldon, S. A. (2008) Targeted development of registries of biological parts. *PLoS One* 3, e2671.
- (12) Knight, T. (2007) The BioBricks Foundation: BBFRFC10, [http://openwetware.org/index.php?title=The\\_BioBricks\\_Foundation:BBFRFC10&oldid=262187](http://openwetware.org/index.php?title=The_BioBricks_Foundation:BBFRFC10&oldid=262187).
- (13) Sauer, R. T. (1978) DNA sequence of the bacteriophage  $\gamma$  *cl* gene. *Nature* 276, 301–302.
- (14) Andersen, J. B., Sternberg, C., Poulsen, L. K., Bjorn, S. P., Givskov, M., and Molin, S. (1998) New unstable variants of green fluorescent protein for studies of transient gene expression in bacteria. *Appl. Environ. Microbiol.* 64, 2240–2246.
- (15) OpenWetWare (2012) *Barcodes - OpenWetWare*, <http://www.openwetware.org/wiki/Barcodes>.
- (16) Kelly, J. R., Rubin, A. J., Davis, J. H., Ajo-Franklin, C. M., Cumbers, J., Czar, M. J., de Mora, K., Gliberman, A. L., Monie, D. D., and Endy, D. (2009) Measuring the activity of BioBrick promoters using an in vivo reference standard. *J. Biol. Eng.* 3, 4.
- (17) Campbell, R. E., Tour, O., Palmer, A. E., Steinbach, P. A., Baird, G. S., Zacharias, D. A., and Tsien, R. Y. (2002) A monomeric red fluorescent protein. *Proc. Natl. Acad. Sci. U.S.A.* 99, 7877–7882.
- (18) Sanger, F., Nicklen, S., and Coulson, A. R. (1977) DNA sequencing with chain-terminating inhibitors. *Proc. Natl. Acad. Sci. U.S.A.* 74, 5463–5467.
- (19) Graham-Rowe, D. (2003) Britain may force DNA 'barcodes' for GM food, <http://www.newscientist.com/article/dn3377-britain-may-force-dna-barcodes-for-gm-food.html>.
- (20) Registry of Standard Biological Parts. *Help: Barcode - partsregistry.org*, <http://partsregistry.org/Help:Barcodes>.
- (21) Schneider, T. D., Stormo, G. D., Yarus, M. A., and Gold, L. (1984) Delila system tools. *Nucleic Acids Res.* 12, 129–140.
- (22) Skulj, M., Okrslar, V., Jalen, S., Jevsevar, S., Slanc, P., Strukelj, B., and Menart, V. (2008) Improved determination of plasmid copy number using quantitative real-time PCR for monitoring fermentation processes. *Microb. Cell Fact.* 7, 6.
- (23) Pribnow, D. (1975) Nucleotide sequence of an RNA polymerase binding site at an early T7 promoter. *Proc. Natl. Acad. Sci. U.S.A.* 72, 784.
- (24) Harley, C. B., and Reynolds, R. P. (1987) Analysis of *E. coli* promoter sequences. *Nucleic Acids Res.* 15, 2343–2361.
- (25) Hook-Barnard, I. G., and Hinton, D. M. (2007) Transcription initiation by mix and match elements: flexibility for polymerase binding to bacterial promoters. *Gene Regul. Syst. Biol.* 1, 275.
- (26) Djordjevic, M. (2011) Redefining *Escherichia coli*  $\sigma(70)$  promoter elements:  $-15$  motif as a complement of the  $-10$  motif. *J. Bacteriol.* 193, 6305–6314.
- (27) Rice, P., Longden, I., and Bleasby, A. (2000) EMBOSS: the European Molecular Biology Open Software Suite. *Trends Genet.* 16, 276–277.
- (28) Campbell, E. A., Muzzin, O., Chlenov, M., Sun, J. L., Olson, C. A., Weinman, O., Trester-Zedlitz, M. L., and Darst, S. A. (2002) Structure of the bacterial RNA polymerase promoter specificity sigma subunit. *Mol. Cell* 9, 527–539.
- (29) Matlock, D. L., and Heyduk, T. (2000) Sequence determinants for the recognition of the fork junction DNA containing the  $-10$  region of promoter DNA by *E. coli* RNA polymerase. *Biochemistry* 39, 12274–12283.
- (30) Mitchell, J. E., Zheng, D., Busby, S. J., and Minchin, S. D. (2003) Identification and analysis of 'extended  $-10'$  promoters in *Escherichia coli*. *Nucleic Acids Res.* 31, 4689–4695.
- (31) Mandeck, W., and Reznikoff, W. S. (1982) A lac promoter with a changed distance between  $-10$  and  $-35$  regions. *Nucleic Acids Res.* 10, 903–912.
- (32) Brosius, J., Erfle, M., and Storella, J. (1985) Spacing of the  $-10$  and  $-35$  regions in the tac promoter. Effect on its in vivo activity. *J. Biol. Chem.* 260, 3539–3541.
- (33) Hook-Barnard, I. G., and Hinton, D. M. (2009) The promoter spacer influences transcription initiation via sigma70 region 1.1 of *Escherichia coli* RNA polymerase. *Proc. Natl. Acad. Sci. U.S.A.* 106, 737–742.
- (34) Straus, D. B., Walter, W. A., and Gross, C. A. (1987) The heat shock response of *E. coli* is regulated by changes in the concentration of  $\sigma 32$ . *Nature* 329, 348–351.
- (35) Lenski, R. E., and Bennett, A. F. (1993) Evolutionary response of *Escherichia coli* to thermal stress. *Am. Nat.* 142, S47–S64.
- (36) Cheung, C., Lee, J., Lee, J., and Shevchuk, O. (2009) The effect of ionic (NaCl) and non-ionic (sucrose) osmotic stress on the expression of  $\beta$ -galactosidase in wild type *E. coli* BW25993 and in the isogenic BW25993 $\Delta$ lacI mutant. *J. Exp. Microbiol. Immunol.* 13, 1–6.
- (37) Reese, M. G. (2000) Computational prediction of gene structure and regulation in the genome of *Drosophila melanogaster*, Ph.D. thesis, University of California Berkeley, Berkeley California, USA/University of Hohenheim, Stuttgart, Germany.
- (38) Reese, M. G. (2001) Application of a time-delay neural network to promoter annotation in the *Drosophila melanogaster* genome. *Comput. Chem.* 26, 51–56.
- (39) Zomer, A. L., Buist, G., Larsen, R., Kok, J., and Kuipers, O. P. (2007) Time-resolved determination of the CcpA regulon of *Lactococcus lactis* subsp. *cremoris* MG1363. *J. Bacteriol.* 189, 1366–1381.
- (40) Gordon, L., Chervonenkis, A. Y., Gammerman, A. J., Shahmuradov, I. A., and Solovyev, V. V. (2003) Sequence alignment

kernel for recognition of promoter regions. *Bioinformatics* 19, 1964–1971.

(41) Bailey, T. L., and Gribskov, M. (1998) Combining evidence using p-values: application to sequence homology searches. *Bioinformatics* 14, 48–54.

(42) Bailey, T. L., and Elkan, C. (1994) Fitting a mixture model by expectation maximization to discover motifs in biopolymers. *Proc. Int. Conf. Intell. Syst. Mol. Biol.* 2, 28–36.

(43) Sambrook, J., and Russell, D. W. (2001) *Molecular Cloning: A Laboratory Manual*, Cold Spring Harbor Laboratory Press, Cold Spring Harbor, NY.

(44) Griffiths, J. (2008) *Griffitts: 5' RACE - OpenWetWare*, [http://openwetware.org/wiki/Griffitts:5%27\\_RACE](http://openwetware.org/wiki/Griffitts:5%27_RACE).

(45) Wilbanks, E. G., Larsen, D. J., Neches, R. Y., Yao, A. I., Wu, C.-Y., Kjolby, R. A. S., and Facciotti, M. T. (2012) A workflow for genome-wide mapping of archaeal transcription factors with ChIP-seq. *Nucleic Acids Res.*, DOI: 10.1093/nar/gks063.

(46) Facciotti, M. T., Pang, W. L., Lo, F. Y., Whitehead, K., Koide, T., Masumura, K., Pan, M., Kaur, A., Larsen, D. J., Reiss, D. J., Hoang, L., Kalisiak, E., Northen, T., Trauger, S. A., Siuzdak, G., and Baliga, N. S. (2010) Large scale physiological readjustment during growth enables rapid, comprehensive and inexpensive systems analysis. *BMC Syst. Biol.* 4, 64.

(47) Griekspoor, A., and Groothuis, T. *4 Peaks, Mekentosj Software*, <http://www.mekentosj.com/science/4peaks>.